High Harmonic Pulse Broadening In An Ionizing Medium

T.E. Glover[1], A.H. Chin[3], and R.W. Schoenlein[2]

[1]*Advanced Light Source Division*
and
[2]*Materials Sciences Division*
Ernest Orlando Lawrence Berkeley National Laboratory
Berkeley, California 94720

[3]*W.W. Hansen Experimental Physics Laboratory*
Stanford University
Stanford, CA 94305

ABSTRACT

High harmonic pulse durations are measured using a laser-and-VUV cross-correlation technique and the results are compared to theory. Harmonic pulses generated using moderate laser intensity are well described by current models and demonstrate that harmonic pulses are temporally broadened when produced at laser intensities sufficiently high to ionize the medium. At even higher generating laser intensity, measured pulse durations are longer than simulated pulse durations. We consider dipole emission from ions and distortion of the spatial laser profile as possible causes for the discrepancy.

PACS numbers: 42.50.Hz, 42.65.Ky, 32.80.Wr

High-order harmonic generation (HHG) has attracted considerable attention as a source of short-pulse (femtosecond), short-wavelength radiation. From a fundamental perspective, HHG is of interest because it requires an understanding of the atom-field interaction in a regime where the electromagnetic field cannot be treated as a small perturbation. From an applications perspective, femtosecond soft x-rays are useful for studying ultrafast material dynamics; in this regard it is important to understand the factors which determine high harmonic pulse durations.

From a theoretical perspective, significant progress has lead to an a priori description of the non-perturbative HHG process [1]. The model of Ref. [1] predicts a complicated dependence of the harmonic yield on laser intensity so that a rich variety of harmonic pulse profiles can result from a given (temporal) laser profile. A number of authors have established that ultrashort pulses are expected from the *single-atom* dipole response [2]. Ultrashort pulses are expected since HHG is a highly non-linear process and since, at high laser intensity, ionization can result in rapid termination of dipole emission : both processes restrict HHG to a narrow window along an already short (typically femtosecond) laser pulse.

Several theoretical studies have accounted for the effects of phase-matching on the harmonic pulse duration [3]. The results depend on whether one-dimensional or three-dimensional phase-matching is considered and upon whether account is taken for ionization. For instance, Salieres *et al.* (considering three-dimensional phase-matching and neglecting ionization) calculate harmonic durations (~60-150 fs) on order of the generating laser pulse duration (150 fs) [3]. In contrast, Kan and co-workers (considering one-dimensional phase-matching and incorporating ionization) calculate pulses which are significantly shorter (~5 fs) than the generating laser duration (150 fs) [3]. In the latter

case, pulse shortening resulted from ionization of the medium which (1) rapidly terminates dipole emission (emission from ions was not considered) and (2) leads to poor phase-matching in the temporal tail of the harmonic pulse (due to the presence of free electrons). These initial theoretical studies suggest that high laser intensity (and associated ionization) lead to ultrashort harmonic pulses.

Experimentally, techniques for measuring femtosecond soft x-ray pulses have only recently been developed [4-6] and careful comparisons between measurement and theory are scarce. Tisch and co-workers [6] have measured the duration of lower order harmonics (13^{th}) and parameterized their measurements with a single effective nonlinearity for harmonic generation. Bouhal and co-workers, working with higher order harmonics (19^{th}) [8], find good agreement with a theory [1] that accounts for the laser-intensity-dependence of this effective nonlinearity. These latter measurements are performed at what we refer to below as 'moderate' laser intensity.

In the present work we use a laser-and-VUV cross correlation technique to measure the duration of high harmonic pulses generated at either 'moderate' or 'high' laser intensity. We find that higher laser intensity leads to longer harmonic pulses. We discuss three principle results of the current investigation. First, at moderate laser intensity measured harmonic pulses are well described by simulations based on the model of Ref. [1]. Second, measured harmonic durations are significantly longer than the expected single-atom pulse duration. Experiment and simulation demonstrate that temporal broadening results when (in an ionizing medium) transverse variations in the generating laser intensity cause time-delayed harmonic emission across the medium. This broadening mechanism, also discussed in [6-8], impedes the generation of ultrashort harmonic pulses and we discuss the degree of transverse variation allowable before

harmonic pulses are significantly broadened. Third, at high laser intensity the measured harmonic pulses are significantly *longer* than the simulated pulses. We consider two factors which may contribute to the discrepancy between measurement and theory : (1) harmonic generation from ions, and (2) distortions of the laser spatial profile.

The laser system used in these experiments is based on titanium-doped-sapphire and provides 800 nm, 110 ±4 fs laser pulses at a repetition rate of 10 Hz [9]. High order harmonics are generated in vacuum by focusing laser pulses (33 μm diameter focal spot) 1.2 cm before the exit of a pulsed-gas-valve backed with argon (~10^{18} atoms/cc output density [10]). Harmonic pulse durations are then measured using a laser-VUV cross-correlation technique discussed in appendix A. Briefly, harmonics are focused to the exit of a second pulsed-gas-valve (backed with helium) along with a 'cross-correlating' laser pulse. Harmonics photoionize helium and the spectrum of photo-emitted electron energies is recorded with a time-of-flight spectrometer. The 'cross-correlating' laser pulse induces changes to the electron energy spectrum; these changes can be used to perform a laser/VUV cross-correlation measurement of the harmonic pulse duration [4]. We estimate that the cross-correlating laser pulse is focused to a spot 5-10 times bigger than the harmonic spot so that we measure the harmonic pulse averaged over the entire harmonic focal spot. Harmonics are generated at either 'moderate' ($2.4^{x}10^{14}$ W/cm^2) or 'high' ($1.1^{x}10^{15}$ W/cm^2) laser intensity. At 'moderate' laser intensity, tunneling ionization rates [10] indicate that (after passage of the laser pulse) the medium is a mixture of both the neutral and singly-ionized species. As discussed below, measurements at 'moderate' intensity are well described by considering harmonic generation solely from the neutral atom (neglecting emission from the ion). At 'high'

laser intensity ionization plays a more important role; ionization states up to $Z=3^+$ are present and we consider harmonic generation from ions.

Harmonic durations discussed below correspond to measurements and calculations for the 25^{th} harmonic of 800 nm (320 Å). Representative cross-correlation curves obtained at the lower and higher laser intensities are shown in Figs. 1 and 2. At low laser intensity the measured cross-correlation is 120±10 fs (Fig. 1) indicating a harmonic pulse which is approximately half the laser duration (50 ±10 fs). When the laser intensity is increased by a factor of four the cross-correlation increases to 157 ±15 fs (Fig. 2) so that the harmonic duration (112 ±15 fs) is approximately equal to the full laser duration. These measurements illustrate that the harmonic generation process is not well described by lowest-order perturbation theory since : (1) the harmonic durations are not equal to the laser duration divided by the square root of the process order [110/√25, as expected for a gaussian laser pulse] and (2) the harmonic durations change with laser intensity [which suggests that the effective process non-linearity is changing with intensity]. To understand these results we calculate high harmonic durations for our experimental conditions.

In order to distinguish single atom from macroscopic effects, we first consider the duration of single atom dipole emission. The atomic dipole response is calculated using the model of Lewenstein and co-workers [1]. This model describes a three-step harmonic generation process : (1) a bound electron tunnels through a laser-suppressed Coulomb barrier, (2) while in the continuum this electron is accelerated by the laser field, causing the electron to gain energy and eventually return to the vicinity of the nucleus, (3) a harmonic photon is produced due to radiative electron-ion capture. Using this model for HHG, we calculate the time-dependent dipole moment resulting from interaction of a

model Ar atom with the laser pulses used in the current experiments. The atom is modeled [1] as a one-electron system subject to a gaussian atomic potential whose ground state binding energy is equal to the ionization potential of Ar. Time-dependent dipole emission is calculated (Eqn. 13 of [1]) at 128 time points per optical cycle and ground state depletion is incorporated using tunneling ionization rates [11]. Specifically, at each time-point the dipole moment is multiplied by a weighting factor equal to the remaining ground state population. The resulting time-dependent dipole moment is Fourier transformed, spectrally filtered to isolate the 25^{th} harmonic, and inverse Fourier transformed to give the harmonic pulse duration.

When ionization is negligible (laser intensity $\leq 10^{14}$ W/cm^2) the harmonic duration is simply the (gaussian) laser duration divided by the square root of the effective process non-linearity (i.e. power law dependence of harmonic yield on laser intensity). While this result is not surprising, it permits a certain richness of harmonic temporal profiles (for a fixed laser temporal profile) because the effective nonlinearity changes with laser intensity. The model in [1] indicates that at low intensity (perturbative harmonic generation) the effective non-linearity for HHG is equal to the process order (25 for the current experiments). At these low intensities, however, the harmonic yield is vanishingly small and the model of Ref. [1] is likely outside its range of validity. With increased laser intensity, one enters the HHG regime : the quasi-free electron appropriate to this regime offers little resistance to absorbing laser photons and the effective non-linearity for HHG becomes less than the process order (we calculate an effective non-linearity of ~6 for the 25^{th} harmonic of 800 nm produced at an intensity of $1.2^{x}10^{14}$ W/cm^2). The reduced non-linearity leads to somewhat longer high harmonic pulses (45 fs given a 110 fs laser) than what would be expected for perturbative harmonic generation (22 fs given a 110 fs laser).

At even higher laser intensity (current experimental conditions), ionization becomes important and harmonic pulses are shortened (compared to 45 fs) due to rapid ionization of the atom [2,3]. Single atom calculations are shown in Figs. 1 and 2 (left insets) and indicate harmonic durations of 20 fs (lower laser intensity) and 10 fs (higher laser intensity) for the current experimental conditions.

The single atom calculations significantly underestimate the measured harmonic durations (50 fs vs. 20 fs at low intensity; 112 fs vs. 10 fs at high intensity) and suggest that macroscopic (phase-matching) effects are important. Accordingly, the 3-dimensional phase-matching integral is calculated; time-dependent dipole emission is calculated over the laser-gas interaction volume and summed in the far-field using a fast Hankel transform algorithm [12]. Account is made for the free-electron-induced modification of the laser and harmonic pulse propagation velocities in the medium [13]. As discussed below, two sets of calculations have been performed. One (left figure 1&2 insets), calculation of the phase-matching integral in a two-dimensional limit (a transverse slice of the medium) for which the dipole moment is calculated as described above for the single-atom calculations. Two (right figure 1&2 insets), calculation of three-dimensional phase-matching for which the dipole moment is calculated using a time-step equal to one laser cycle. Accordingly, laser-cycle-averaged expressions for the tunneling ionization rate [11] and the dipole moment (Eqn. 22 Ref[1]) are used for the three-dimensional calculations. A comparison of the left vs right figure (1&2) insets indicates that the primary pulse shaping mechanisms discussed below are already evident in the two-dimensional calculations and that using a larger time-step (1 cycle vs $1/128^{th}$ of a cycle) does not significantly alter the harmonic pulse envelope.

When three-dimensional phase-matching is included in the simulations the calculated (lower intensity) pulse duration broadens from 20 fs to 50 fs (Fig. 1 left inset). Significantly, the calculated harmonic duration is in good agreement with the measured pulse duration (50 fs). The temporal broadening associated with calculation of the phase-matching integral is due to time-delayed harmonic generation across the medium (discussed below) and has been observed in the experiments of [6,8] and the calculations of [7].

The measurements of Fig. 1 indicate that the model of Ref. [1] accurately describes harmonic pulses when account is made for the phase-matching process. We separate phase-matching into a consideration of longitudinal effects (representing the finite length of the medium along the laser propagation direction) and transverse effects (representing the transverse extent of the medium). For the current experimental conditions, our simulations indicate that transverse effects dominate the harmonic profile (compare left vs right insets of figures 1&2). For the current focusing conditions (z/z_r ~10) the ratio of the longitudinal co-ordinate (z) to the Rayleigh range (z_r) changes by only ~10-20% over the length of the medium (1-2 mm). Accordingly, pulse shaping effects associated with 'longitudinal' phase-matching are mild since amplitude and phase variations of the laser along the medium are relatively small.

Pulse broadening associated with the finite *transverse* extent of the medium results from a combination of two factors : (1) transverse intensity variations across the laser focal spot and (2) ionization of the medium in the presence of transverse intensity variations. The first factor is, even in the absence of ionization, important since the effective non-linearity for HHG varies with laser intensity. Accordingly, harmonic generation will be dominated by emission from a narrow range of transverse coordinates

(in the medium) determined by two factors : how fast the harmonic yield decays with decreased laser intensity and how fast the laser intensity decays with increased transverse coordinate. To understand broadening from factor (2) one can think of HHG as occurring over a fixed range of laser intensities : it begins at a threshold (so called 'cutoff') intensity and ends when an atom is ionized. A transverse variation in the generating laser intensity causes the harmonic generating intensity interval to occur at different times across the transverse profile of the medium. Harmonics on axis are created on the leading edge of the laser pulse (at early time) while harmonics created off axis are produced at late time and broaden the harmonic pulse.

In order to explicitly demonstrate that harmonic temporal broadening results from time-delayed harmonic generation across the medium, harmonics were measured using a laser pulse with limited transverse intensity variation. The harmonic generating laser beam was clipped by an aperture at $0.5*\omega$ and imaged into the Ar gas jet (ω is the beam radius). The laser spatial profile, viewed on a camera at an image plane equivalent to that of the gas jet, was observed to be gaussian with a hard edge at $0.5*\omega$. The resulting cross-correlation measurement obtained at low laser intensity (Fig. 1, 110 $\pm$10 fs) indicates that aperturing the beam has reduced the harmonic pulse duration from 50 fs to $\leq$40 fs (resolution limited). We calculate a harmonic duration of 40 fs for these aperturing conditions. Additionally the correlation is observed to shift in time away from the temporal peak of the generating laser pulse, an effect consistent with reduction of late-time harmonic generation in the spatial wings of the laser pulse. Similar results are obtained when the laser intensity is increased (discussed below).

We next consider the amount of transverse variation allowable before the pulse broadening mechanisms discussed above become significant. Harmonic pulse broadening

is most severe when ionization accompanies transverse laser intensity variations and will depend on the nature of the intensity variation. The laser systems typically used for HHG produce spatially gaussian beams; we therefore consider the effects of aperturing a gaussian beam at different levels (non-gaussian profiles are considered below). Given a gaussian laser focal spot, harmonic broadening does not change with spot size since (as long as the laser is contained within the medium) the functional form of the transverse variation is unchanged. An *apertured* gaussian profile confines harmonic emission to a small on-axis portion of the medium, limiting the degree of transverse intensity variation. Simulations (performed at 10^{15} W/cm^2) indicate that transverse temporal broadening is negligible if a gaussian laser profile is apertured at 0.25*ω. At this point 60% of the laser energy has been apertured and transverse intensity variations have been reduced to ~10%.

Finally, we discuss the measurements performed at high laser intensity. At high intensity we observe a discrepancy between measurement and theory; measured pulse durations are significantly longer than calculated pulse durations. A cross-correlation measurement performed at the higher (generating) laser intensity and using a (full) gaussian spatial profile is shown in Fig. 2. The least squares gaussian fit to the correlation curve is 157 ±15 fs, indicating a (gaussian) harmonic duration of 112 ±15 fs. Figure 2 (right inset) shows the calculated harmonic pulse; the pulse is asymmetric due to variations in harmonic generation efficiency across the transverse profile of the laser focal spot and the (full width at half maximum) pulse duration is 65 fs. The discrepancy between measured and calculated harmonic durations persists for the second set of measurements performed using the apertured laser beam and the higher intensity (measured harmonic duration of 73 ±15 fs, simulated duration of 30 fs).

The cause of the discrepancy between measured and calculated harmonic profiles is unknown. We consider two factors which may contribute to the harmonic pulse broadening we observe at high laser intensity. First, harmonic generation from ions and second, the effects of distortion of the (spatial) transverse laser profile.

First we consider the influence of dipole emission from ions. One can anticipate that Ar will experience significant ionization at high laser intensity (1.1×10^{15} W/cm^2) since the threshold for complete laser suppression of the Coulomb barrier is 2.4×10^{14} W/cm^2 [14]. We use tunneling ionization rates [11] to calculate ionization over the three-dimensional interaction region and find that (at a peak intensity of 1.1×10^{15} W/cm^2) the medium is predominantly doubly-ionized by the end of the laser pulse. We therefore calculate harmonic dipole emission from the relevant ionization states of Ar.

At fixed laser intensity, dipole emission from an ion species should be weaker than emission from the neutral since the electron is more tightly bound in the ion (i.e. the ion is less polarizable). While weaker ion-dipole-emission at *fixed* laser intensity is intuitive, ions also survive to higher laser intensity (an effect which offsets the lower polarizability). Given these two opposing factors, it is not intuitively obvious which dominates. We calculate dipole emission at the 25th harmonic using the model of Ref. [1] (Eqn. 22) and noting that the ionization potential is the sole parameter which characterizes a given atom/ion. Calculated single-atom dipole emission strengths for neutral through triply-ionized Ar are shown in Fig. 3. As indicated in Fig. 3, our simulations indicate that the emission strength for the ion species is orders of magnitude lower than for the neutral. These simulations suggest that the decreased ion polarizability is more important than the increased survivability to high laser field strength.

The results of Fig. 3 suggest that dipole emission from ions will not significantly alter the harmonic temporal profile. We have incorporated the calculations of Fig. 3 into the three-dimensional phase-matching simulations; account is made for time-dependent ionization and harmonic emission from the various ion states (up to $z=5^{+}$). We find that while significant ionization (up to $z=3^{+}$) can occur over the medium, harmonic pulse profiles are not significantly affected by dipole emission from ions owing to weak ion emission strength.

In contrast to the relative emission strengths suggested by Fig. 3, we note that numerical simulations by Krause, Schafer and Kulander indicate that dipole emission from ions can be comparable to that from the neutral [15]. The simulations of [15] are based on numerical evaluation of the time-dependent Schroedinger equation and indicate that the harmonic yield (square of the dipole emission strength) is proportional to the ionization rate of the given atom/ion. Accordingly, dipole emission from an ion species can be comparable to that of the neutral if the two species have comparable peak ionization rates. This scaling with intensity reflects the fact that both harmonic generation and ionization require excitation out of the ground state. While we are uncertain as to the origin of the discrepancy between the numerical results of [15] and our simulations based on the analytic results of [1], we attempt to assess our pulse duration measurements in light of the conclusions reached by Krause, Schafer and Kulander.

Harmonic pulse durations are re-calculated with account taken for dipole emission from ions; now, however, the dipole emission strength is set equal to a constant times the (time-dependent) ionization rate of the atom/ion of interest. Figure 4 shows time-dependent (tunneling) ionization rates for neutral through doubly-ionized Argon : we plot the product of the on-axis ionization rate and the population which sees this ionization

rate as a measure of the peak ionization rate seen by a given ion-stage (at the *center* of the medium; i.e. peak laser field). We see that the peak ionization rate of the singly-charged ion is comparable to that of the neutral (~15% difference) so that the two will have comparable dipole emission at the center of the medium (given the scaling suggested in [15]). The doubly-charged ion sees a lower peak ionization rate because the laser intensity is too low to saturate ionization for the doubly-charged ion.

While Fig. 4 indicates that ion and neutral dipole emission can be comparable at medium center, it is the emission averaged over the interaction volume which is of interest. In this averaging process the neutral will once again exert its dominance; the volume over which the neutral emits is larger than the volume over which the single-ion emits (which in turn is larger than the volume over which the double-ion emits). Our three-dimensional calculations perform this spatio-temporal averaging. Upon performing this simulation (three-dimensional harmonic generation with account taken for ion-dipole-emission and the dipole strength set equal to the ionization rate), we observe a 15% increase in the 'high-intensity' harmonic pulse duration (from 65 to 75 fs). This increase is modest because neutral Argon dominates the dipole emission volume. We conclude that while dipole emission from ions may play some role in explaining the discrepancy between measurement and theory observed at high laser intensity, it does not account for the entire discrepancy.

We next consider distortion of the transverse laser-beam profile. Efficient generation of short-wavelength high harmonic radiation requires high laser intensity since the short-wavelength cutoff for HHG varies linearly with laser intensity (up to the ionization threshold and assuming harmonic photon energies large compared to the binding energy of the atom). At such high intensity, laser-plasma interactions can distort

the spatial profile of the generating laser pulse. These distortions can, in turn, alter the harmonic temporal profile. Various mechanisms for laser distortion have been discussed in the literature [16]. For instance, the transverse variation in laser intensity combined with ionization of the medium creates an electron density profile which acts as a negative lens and can lead to laser beam refraction [Rankin, 16]. For the current experimental conditions we calculate [16] that the characteristic length over which beam refraction becomes significant is ~0.7 mm (compared to the 1-2 mm medium length) so that the effects of beam refraction are not negligible. Similarly beam break-up (filamentation) due to self-focusing has also been observed in high-intensity laser-plasma interaction [17]. A detailed analysis of plasma-induced laser distortion is beyond the scope of this paper. Instead we calculate harmonic temporal profiles given a few non-gaussian transverse laser profiles.

Varying the functional form of the laser focal spot can alter the harmonic temporal profile because it alters how time-delayed harmonic generation occurs across the medium. Experiments (at high intensity) have been performed using a gaussian focal spot (harmonic duration of 112 fs) and using a clipped gaussian (73 fs). Clipping the gaussian minimizes the time interval over which harmonics are produced across the medium and leads to shorter pulses. Similarly laser focal spots whose functional form produces more rapid intensity variation (than a gaussian) should also lead to shorter harmonic pulses. Simulations using a squared gaussian transverse laser profile indicate that harmonic pulse durations are reduced by ~40% (compared to a gaussian). Conversely, functional forms which reflect a slower transverse intensity variation produce longer harmonic pulses. Simulations indicate that a square-root gaussian laser focal spot produces harmonic pulses which are 25% longer than obtained using a gaussian laser spot (calculations

assume a peak intensity of $1.1^{x}10^{15}$ W/cm^2; calculated pulse is shown in Fig. 5). Ionization-induced laser beam defocusing should produce a slower transverse intensity variation since the effect of refraction is to enlarge the beam (increase the gaussian beam waist). Given ideal defocusing, however, an initially gaussian beam will remain gaussian so that additional non-linearities are required to produce a non-gaussian beam (and therefore an altered harmonic pulse duration).

Finally, we have considered a sinusoidally modulated gaussian laser profile with modulation periods of 1 and 100 μm. A modulated gaussian can be taken to reflect some aspects of beam filamentation and self-focusing. A high-frequency modulation is observed to produce modulations on the harmonic pulse (which is also shortened by ~65%) while the low-frequency modulation has a smaller effect on the harmonic pulse (30% shortening, Fig. 5).

The simulations of Fig. 5 are intended to illustrate that laser beam distortion can alter the harmonic temporal profile and that such beam distortion may contribute to the discrepancy between measurement and theory observed at high laser intensity. A detailed quantitative analysis of this effect is beyond the scope of the current investigation. We note, however, that the experimental task is non-trivial; it is important to characterize the spatio-temporal evolution of the laser *throughout* the plasma (since harmonics are generated throughout the plasma), not simply after it has exited the plasma.

In Conclusion, high-order harmonic generation is characterized by a dependence upon laser intensity of both the effective process non-linearity and the phase of the generated polarization. These dependencies produce a rich variety of harmonic pulse durations for a given laser duration. Laser-and-VUV cross-correlation measurements in combination with simulations elucidate some of the factors important to determining the

harmonic duration. Experiments are performed in a weak focusing regime in order to better isolate amplitude effects (variations in effective non-linearity or ionization rate) from true phase-matching effects (variations in the phase of the laser or non-linear polarization). Measured harmonic durations are significantly longer than expected from single atom calculations and can be understood as resulting predominantly from amplitude effects. To summarize we consider three regimes of laser intensity. At low (non-ionizing) intensity the harmonic duration is determined by the effective non-linearity for HHG as averaged across the medium. At higher (ionizing) laser intensity transverse variations in the laser focal spot are important and lead to significant harmonic pulse broadening due to time-delayed harmonic emission across the medium. Our results suggest that significant harmonic pulse shortening can be achieved by using an approximately flattop laser profile (variations ≤10%) in combination with high (ionizing) laser intensity. Finally, at the highest laser intensity used, measured pulse durations are longer than simulated. We speculate that harmonic generation from ions combined with plasma-induced distortion of the laser pulse can contribute to additional harmonic pulse broadening.

The authors are thankful for enlightening discussions with and equipment loans from C. V. Shank, G. Cerullo, T. D. Donnelly, A. M. Goetz, R.W. Falcone, R.R. Freeman, M.D. Perry and L.B. Da Silva. This work is supported by the Department of Energy under contract AC03-76SF00098.

Appendix A : Experimental Method

The laser system used in these experiments is based on titanium:sapphire and delivers ~100 fs, 800 nm pulses at a 10 Hz repetition rate. The laser intersects a beamsplitter (Fig. A1); one beam is used to generate harmonic radiation while the other beam is directed out of a vacuum chamber, through an optical delay arm and then propagated back into vacuum for subsequent spatial and temporal overlap with the harmonic radiation. High order harmonics are generated using a 50 cm focal-length curved-mirror which focuses the laser to a 33 μm diameter focal spot. The transverse laser profile in the Ar interaction region is measured at an equivalent image plane using leakage (~1%) through the curved mirror and a CCD camera.

A pulsed-gas-valve (1 mm valve orifice) positioned 1.2 cm beyond the laser focal spot is backed with Argon and delivers an output gas density of $\sim 10^{18}$ atoms/cc. High order harmonics generated from the laser-Ar interaction pass through a 1500 Å thick Aluminum filter (which eliminates 800 nm radiation) and propagate ~2 m to a Mo:Si multilayer-coated curved mirror. The multilayer (peak reflectivity of 22% at 38 eV and 4 eV FWHM bandpass) focuses soft x-ray pulses to the exit of a second pulsed-gas-valve backed with Helium. We estimate that the focused x-ray spot diameter is 20 μm. The output pressure of the He gas jet (between 0.1 and 1 Torr) is adjusted to obtain the maximum signal level without creating significant space charge broadening of the photoelectron peaks. Photoelectrons generated by soft x-ray ionization of He are collected by a pair of flight-time-preserving reflecting parabolic grids [18]. The grids collect electrons over ~4π and direct them along a 1m flight tube to a microchannel plate detector. Electron energies are recorded via time-of-flight spectroscopy using a 2 Gs, 500

MHz digitizing oscilloscope. A representative photoelectron spectrum is shown by the dashed curve of Fig. A1. Nominally three-peaks are present since the multi-layer mirror transmits ~3 harmonics; the 25^{th} harmonic appears at ~ 15 eV.

Modifications to the photoelectron spectrum are induced using a second 800 nm laser pulse which is sent through an optical delay arm. This perturbing laser pulse is focused (at f/67; 450 μm focal spot diameter) into the He interaction region through a 4 mm diameter hole in the multilayer mirror. The temporal width of the perturbing laser pulse is measured using a single-shot auto-correlator and this laser pulse is overlapped in space and time with the harmonic pulse in the He interaction region. Spatio-temporal overlap is achieved as follows : the Al filter is rotated to allow transmission of the harmonic-generating laser pulse. This laser pulse is focused (by the multi-layer mirror) into the He interaction region along with the perturbing laser pulse. The He interaction region is then imaged (using a single lens) out of vacuum and onto a non-linear crystal (KDP). The perturbing laser pulse is then adjusted in space and time to produce (in combination with the harmonic-generating laser pulse) sum-frequency generation in the KDP crystal. The production of sum-frequency generation indicates that the harmonic and perturbing-laser pulses are overlapped in the He interaction region. We find this procedure to be an efficient and accurate way to achieve spatio-temporal overlap.

A representative laser-perturbed spectrum is shown by the solid curve of Fig. A1. Additional photoelectron peaks arise due to scatter of optical photons. Laser-harmonic cross-correlation curves are obtained by measuring the amplitude of an optical-scattering-peak as a function of harmonic/laser relative time-delay. It is desirable to measure cross-correlation curves in a regime where the optical scattering peak amplitude varies linearly with laser intensity (or nearly so). In this regime deconvolution of the harmonic duration

from the cross-correlation curve is straight forward; otherwise on must carefully measure the laser intensity dependence of the optical scattering process (i.e. the saturation behavior of the scattering process).

The manner in which first-order optical scattering saturates is shown in Fig. A2. Optical scattering probabilities are calculated using the following expression [4] for the probability, P_n , that the photoelectric effect is accompanied by absorption (n>0) or emission (n<0) of n laser photons :

$$P_n = (3/2)\cdot(p/p_o)^3\cdot[\{1+(a/h)^2\cdot p_o^2\}/\{1+(a/h)^2\cdot p^2\}]^4\cdot\int_o^{\pi} \sin(\Theta)\cdot\cos^2(\Theta)J_n^2(\alpha,\beta)\, d\Theta \quad (A1)$$

In (A1), a is the Bohr radius divided by the nuclear charge; h is planck's constant divided by 2π; the momenta, p_o and p, are $p=[2m(h\nu_x + n\cdot h\nu - E_b - U_p)]^{0.5}$ and $p_o=[2m(h\nu_x - E_b)]^{0.5}$ where m is the electron mass, $h\nu_x$ is the harmonic photon energy, $h\nu$ is the laser photon energy, E_b is the field free binding energy and U_p is the ponderomotive potential of the laser [19]. The generalized Bessel function, $J_n(\alpha,\beta)$, is discussed in [19] and its arguments are $\alpha = e\cdot A_o\cdot p\cdot\cos(\Theta)/(mch\nu)$, $\beta = -U_p/2\cdot h\nu$ where e is the electron charge and A_o is the vector potential of the laser.

First-order optical scattering is shown in Fig. A2. In constructing Fig. A2, we have calculated the probability for scattering (absorbing or emitting) one laser photon as a function of laser intensity. Calculated optical scattering probabilities are then parameterized by a power law dependence upon laser intensity (scattering probability ~ I^q; I=laser intensity, q=a parameter). The power-law exponent, q, therefore represents the effective non-linearity for first-order optical scattering. This effective non-linearity changes with laser intensity (or equivalently with optical scattering probability) and represents whether a laser/harmonic cross-correlation is performed in a linear (q~1) or saturated (q<<1) regime. Inspection of Fig. A2 illustrates that optical scattering can be

easily saturated, with a 10% optical scattering probability giving an effective non-linearity of ~0.85. This is a modest level of saturation and corresponds to an effective laser-pulse broadening of ~10% ($\tau_{laser}/\sqrt{0.85} = 1.085*\tau_{laser}$; assuming a gaussian laser pulse). Cross-correlation measurements in the current experiments are performed at an optical scattering probability of ~5%; here the effective non-linearity is 0.93 and leads to an effective increase in the laser duration of 4 fs. As indicated in Fig. A2, care must be taken to measure (the somewhat complicated) saturation behavior of the optical scattering process if measurements are performed in a regime 'strong' optical scattering.

References

[1] M. Lewenstein, *et al.*, Phys. Rev. A **49**, 2117 (1994).

[2] P.B. Corkum, *et al*., Opt. Lett. 19, 1870 (1994); Philippe Antoine, *et al.*, Phys. Rev. A **51**, R1750 (1995); I.P. Christov, *et al.*, Phys. Rev. Lett. **78**, 1251 (1997); and references therein.

[3] Pascal Salieres, *et al.*, Phys. Rev. Lett. **81**, 5544 (1998); C. Kan *et al.*, Phys. Rev. Lett. **79**, 2971 (1997); Philippe Antoine, *et al.*, Phys. Rev. A **56**, 4960 (1997); Pascal Salieres, *et al.*, Phys. Rev. Lett. **74**, 3776 (1995); C. Kan, *et al*., Phys. Rev. A **52**, R4336 (1995).

[4] T.E. Glover, *et al*., Phys. Rev. Lett. **76**, 2468 (1996).

[5] J. M. Schins, *et al.* , Phys. Rev. Lett. **73**, 2180 (1994); J.M. Schins, *et al.* J. Opt. Soc. Am. B **13**, 197 (1996); A. Bouhal, *et al.*, J. Opt. Soc. Am. B **14**, 950 (1997); Y. Kobayashi *et al.*, Opt. Lett. 21, 417 (1996).

[6] J.W.G. Tisch et al., Phys. Rev. Lett. **80**, 1204 (1998).

[7] J.E. Muffett J. Phys. B **27**, 5693 (1994); T. Ditmire : J. Opt. Soc. Am B **13**, 406 (1996).

[8] A. Bouhal *et al.*, Phys. Rev. A **58**, 389 (1998).

[9] The laser profile is least-squares fit to a two component gaussian : 110 fs (main pulse) plus a 3% (by amplitude) 525 fs gaussian (temporal wings).

[10] T. E. Glover, Ph.D. thesis, University of California at Berkeley (1993); T. Adachi, *et al.*, Appl. Phys. B **55**, 1786 (1992); M.D. Perry *et al.*, Optics Letters **17**, 7 (1992).

[11] Gibson *et al.* Phys. Rev. A 41, 5049 (1990); M. Ammosov,*et al*., Sov. Phys. JETP. **64**, 1191 (1986).

[12] V. Magni, G. Cerullo, S. DeSilvestri, J. Opt. Soc. Am B **9**, 2031 (1992); A.E. Siegman, Opt. Lett. **1**, 13 (1997).

[13] M.E. Faldon, et al., J. Opt. Soc. Am. B **9**, 2094 (1992).

[14] S. Augst, *et al*., Phys. Rev. Lett. **63**, 2212 (1989).

[15] Jeffrey L. Krause, Kenneth J. Schafer, and Kenneth C. Kulander, Phys. Rev. Lett. **68**, 3535 (1992).

[16] A.B. Borisov, *et al.*, Phys. Rev. Lett. **68**, 2309 (1992); T. M. Antonsen, *et al.*, Phys. Rev. Lett. **69**, 2204 (1992); R. Rankin, *et al.*, Opt. Lett. **16**, 835 (1991).

[17] P. Sprangle, *et al*., Phys. Rev. A **41**, 4463 (1990).

[18] D.J. Trevor, L.D. Van Woerkom, and R.R. Freeman, Rev. Sci. Instrumen. **60**, 1051 (1989).

[19] Howard R. Reiss, Phys. Rev. A **22**, 1786 (1980).

Figure Captions

Figure. 1 Measurements and calculations for generating the 25th harmonic of 800 nm using a peak laser intensity of 2.4x10^{14} W/cm^2. Four results are displayed. First (main figure) : measured cross-correlation between the harmonic pulse and a 110 fs laser pulse. A least-squares gaussian fit (solid curve, 120 ±10 fs) to the data (solid diamonds) indicates a harmonic duration of 50 ±10 fs. Second (left inset) : calculated single atom harmonic pulse (solid curve, 20 fs) and the harmonic pulse obtained when account is taken for the transverse extent of the medium (dashed curve, 50 fs). Third (right inset) : harmonic durations calculated with account taken for the transverse and longitudinal extent of the medium assuming a gaussian laser focal spot of radius ω (solid curve, 50 fs) and a gaussian focal spot apertured at 0.5*ω (short-dashed curve 40 fs). The laser pulse (long-dashed curve) is also shown. Finally (main figure), the measured laser-and-harmonic cross-correlation (data : hollow diamonds; gaussian fit of 107 ±10 fs : dashed curve) obtained using a laser spot apertured at 0.5*ω indicating a harmonic duration of ≤40 fs (resolution-limited).

Figure. 2 Measurements and calculations for generating the 25th harmonic of 800 nm using a peak laser intensity of 1.1x10^{15} W/cm^2. Four results are displayed. First (main figure) : measured cross-correlation between the harmonic pulse and a 110 fs laser pulse. A least-squares gaussian fit (solid curve, 157 ±15 fs) to the data (solid diamonds) indicates a harmonic duration of 112 ±15 fs. Second (left inset) : calculated single atom harmonic pulse (solid curve, 10 fs) and the harmonic pulse obtained when account is taken for the transverse extent of the medium (dashed curve, 70 fs). Third (right inset) : harmonic durations calculated with account taken for the transverse and longitudinal extent of the medium assuming a gaussian laser focal spot of radius ω (solid curve, 65 fs) and a gaussian focal spot apertured at 0.5*ω (short-dashed curve, 30 fs). The laser pulse (long-dashed curve) is also shown. Finally (main figure), the measured laser-and-harmonic cross-correlation (data : hollow diamonds; gaussian fit of 132 ±15 fs : dashed

curve) obtained using a laser spot apertured at $0.5*\omega$ indicating a harmonic duration of 73 ±15 fs.

Figure 3. Dipole emission strength (dipole amplitude squared) vs laser intensity for the 25^{th} harmonic of 800 nm as generated from various ionization states of Argon : Neutral (solid line), singly-ionized (short-dashed line), doubly-ionized (long-dashed line), triply-ionized (circles). The calculations are based on Eqn. 22 of Ref. [1].

Figure 4. Time-dependent ionization rates for neutral (solid), singly-ionized (short-dashes), and doubly-ionized (long-dashes) Argon. The left axis is the ionization rate of a given ion species multiplied by the population of that ion stages (at the center of the medium). The inset shows the ionization rate (left axis, solid curve) and population (right axis, dashed curve) curves individually for neutral Argon. Tunneling ionization rates are used (Ref [10]).

Figure 5. Calculated harmonic temporal profiles for different transverse (spatial) laser profiles : gaussian profile (open circles with dashed line, FWHM 65 fs), square-root gaussian (solid line, FWHM 80 fs), and sinusoidal modulation at 100 um period (dashed line, FWHM 22 fs). Inset : gaussian profile (dashed line) and sin modulation at 1um period (solid line, FWHM 45 fs). A peak laser intensity of $1.1x10^{15}$ W/cm^2 is assumed.

Figure A1. Experimental arrangement. High order harmonics are generated by focusing 800 nm laser pulses (using a 50 cm focal-length curved mirror) ~1cm before the exit of a pulsed-gas-valve backed with Ar. An Al filter blocks the 800 nm radiation and allows harmonic radiation to propagate to a Mo:Si multilayer-coated mirror. The multi-layer optic focuses high harmonic radiation to a second pulsed-gas-valve backed with He. The

harmonics photoionize He and the spectrum of photoelectron energies is analyzed via time-of-flight. A representative photoelectron spectrum is shown by the dashed curve (harmonics 23 through 27 contribute to the spectrum). The photoelectron spectrum is perturbed using a second, time-delayed, laser pulse which is overlapped in space and time with the harmonic pulse in the He interaction region. The laser perturbed spectrum is shown by the solid curve indicating additional peaks due to scatter of optical photons. Several diagnostics are indicated : (1) a camera views the harmonic generating laser focal spot at an image plane equivalent to that in the Ar interaction region; (2) a single-shot correlator measures the cross-correlating laser pulse width; (3) spatio-temporal overlap is achieved by using a lens to image the He interaction region into a non-linear crystal (KDP). In this last diagnostic, the Al filter is removed (rotated) and the two 800 nm laser pulses are spatially and temporally overlapped in a KDP crystal (produce sum frequency generation from the two beams). Since the KDP crystal is at an image plane, the two beams are therefore also spatio-temporally overlapped in the He interaction region. The *harmonic* and perturbing laser pulses are therefore overlapped in the He interaction region.

Figure A2. Effective non-linearity for scattering one laser photon vs optical scattering probability. The laser-intensity dependence for first-order optical scattering is parameterized as a constant times the laser intensity to some power, q. The power-law exponent, q, represents the effective non-linearity of the optical scattering process. This effective non-linearity is displayed as a function of the (first order) optical scattering probability and indicates whether optical scattering occurs in a linear ($q\sim1$) or saturated ($q<<1$) regime.

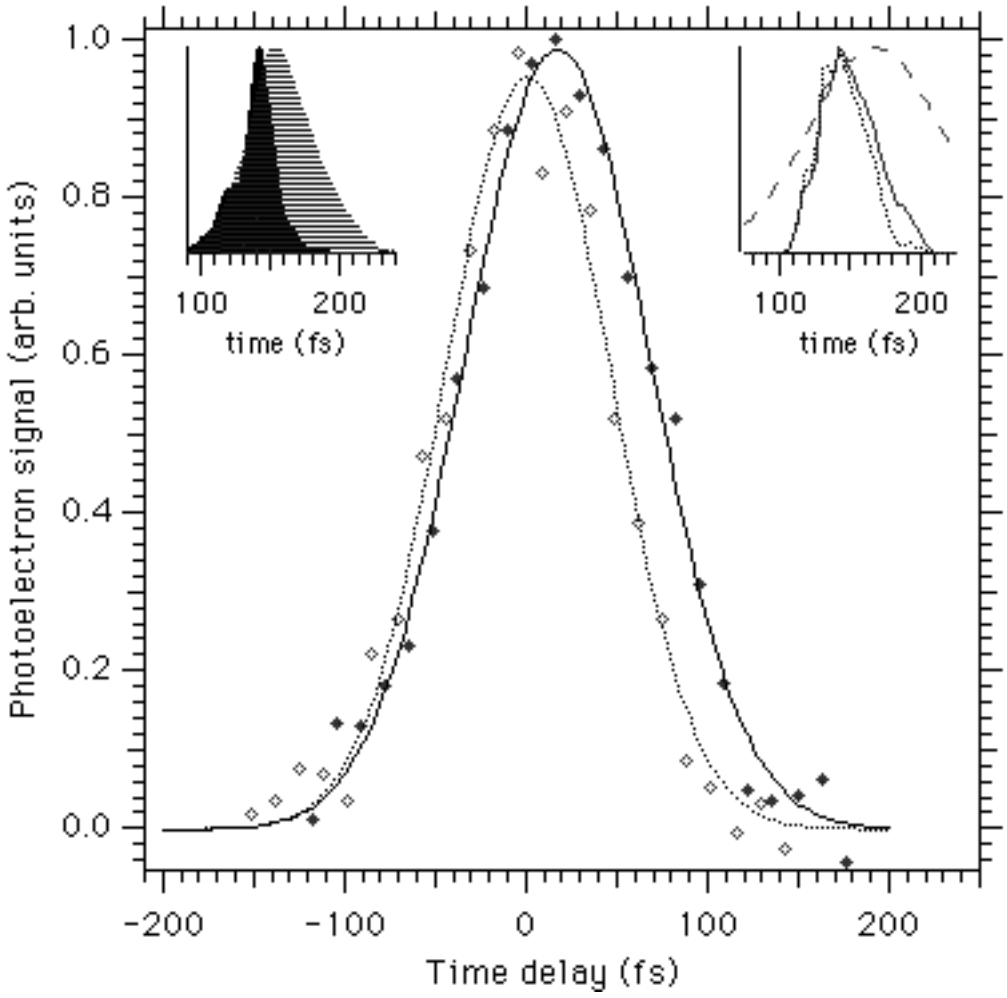
Photoelectron signal (arb. units)
1.0
0.8
0.6
0.4
0.2
0.0
-200
-100
0
100
200
Time delay (fs)
100
200
time (fs)
100
200
time (fs)

Figure 1

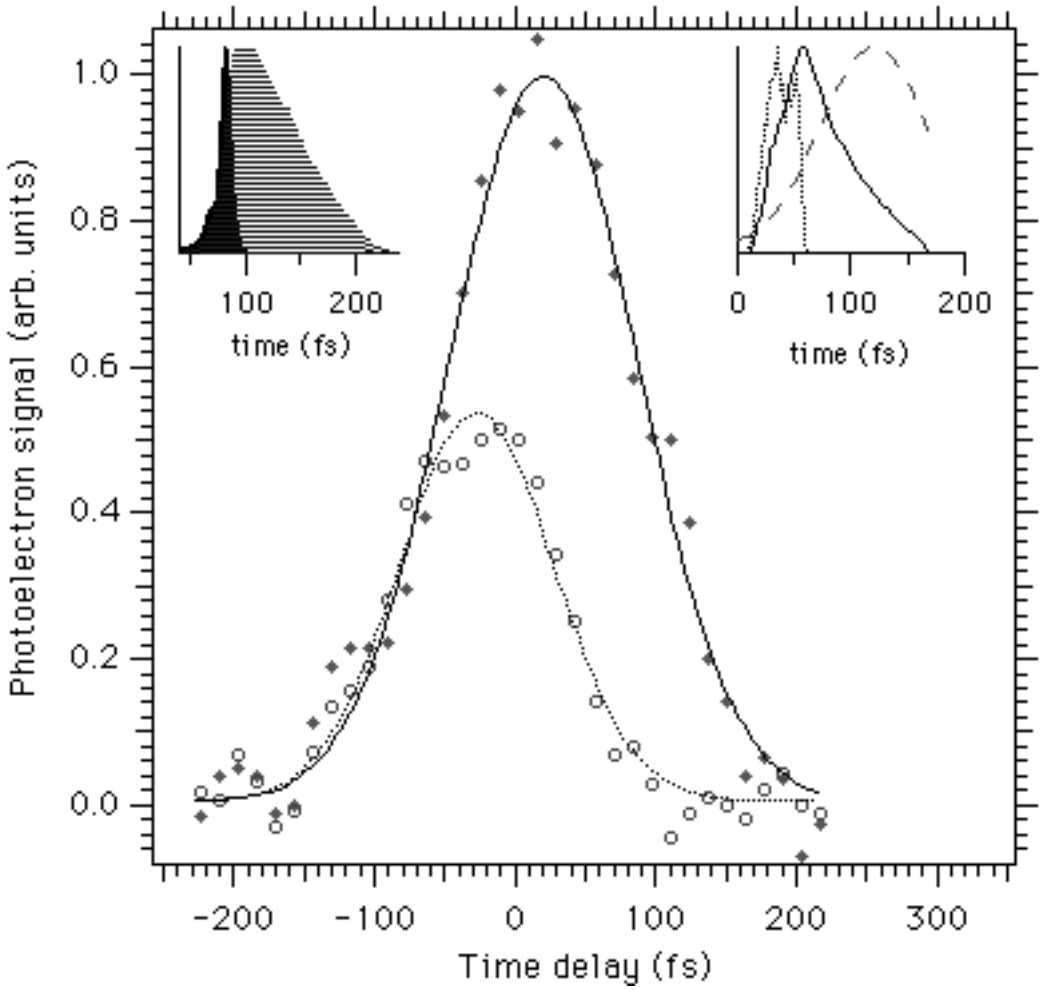
Photoelectron signal (arb. units)
1.0
0.8
0.6
0.4
0.2
0.0
-200
-100
0
100
200
300
Time delay (fs)
100
200
time (fs)
0
100
200
time (fs)

Figure 2

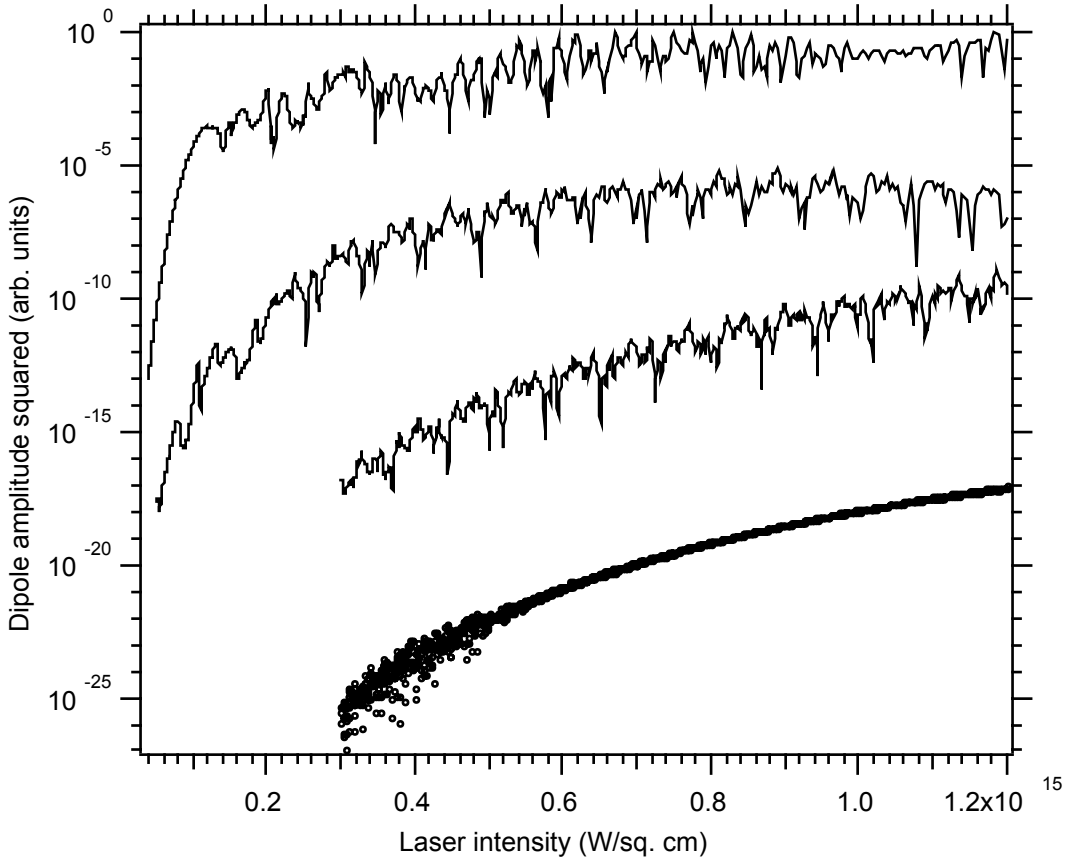
Dipole amplitude squared (arb. units)
10 0
10 -5
10 -10
10 -15
10 -20
10 -25
0.2
0.4
0.6
0.8
1.0
1.2x10 15
Laser intensity (W/sq. cm)

Figure 3

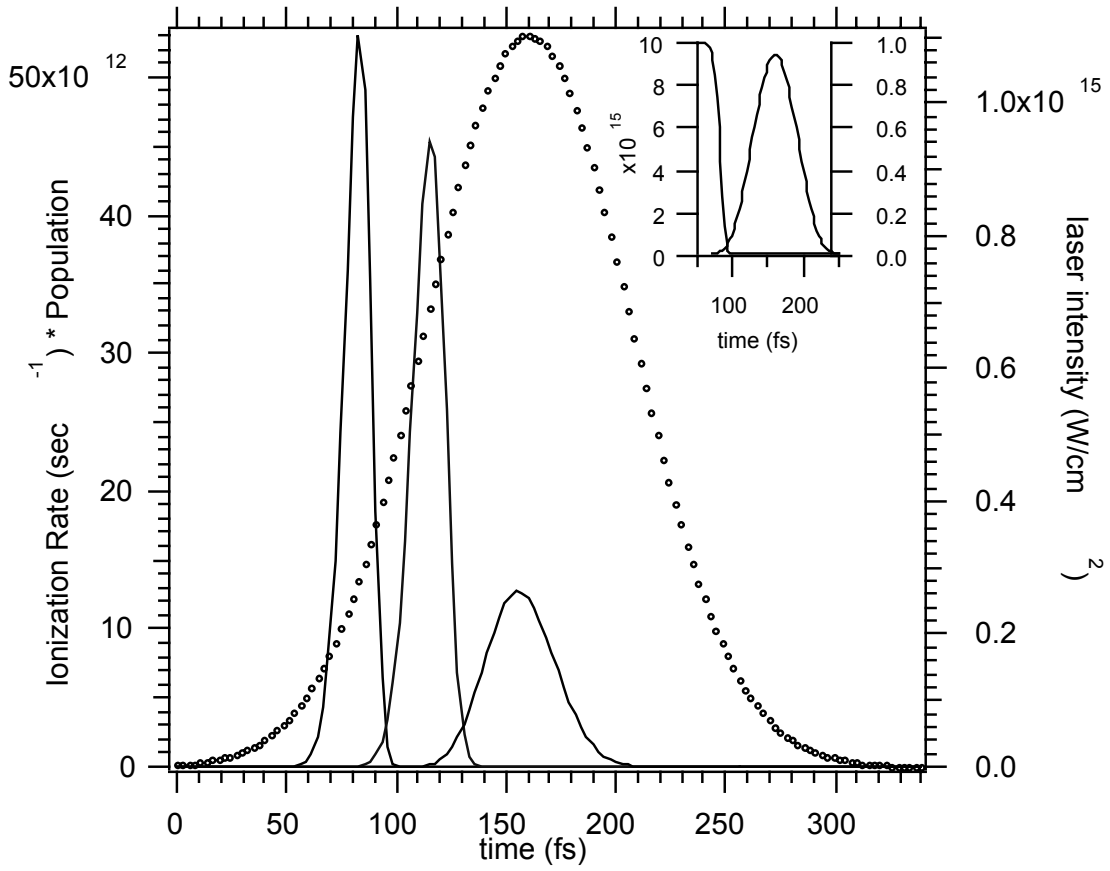
50x10 12
40
30
20
10
0
Ionization Rate (sec -1) * Population
0
50
100
150
200
250
300
time (fs)
1.0x10 15
0.8
0.6
0.4
0.2
0.0
laser intensity (W/cm 2)
10
8
6
4
2
0
x10 15
1.0
0.8
0.6
0.4
0.2
0.0
100
200
time (fs)

Figure 4

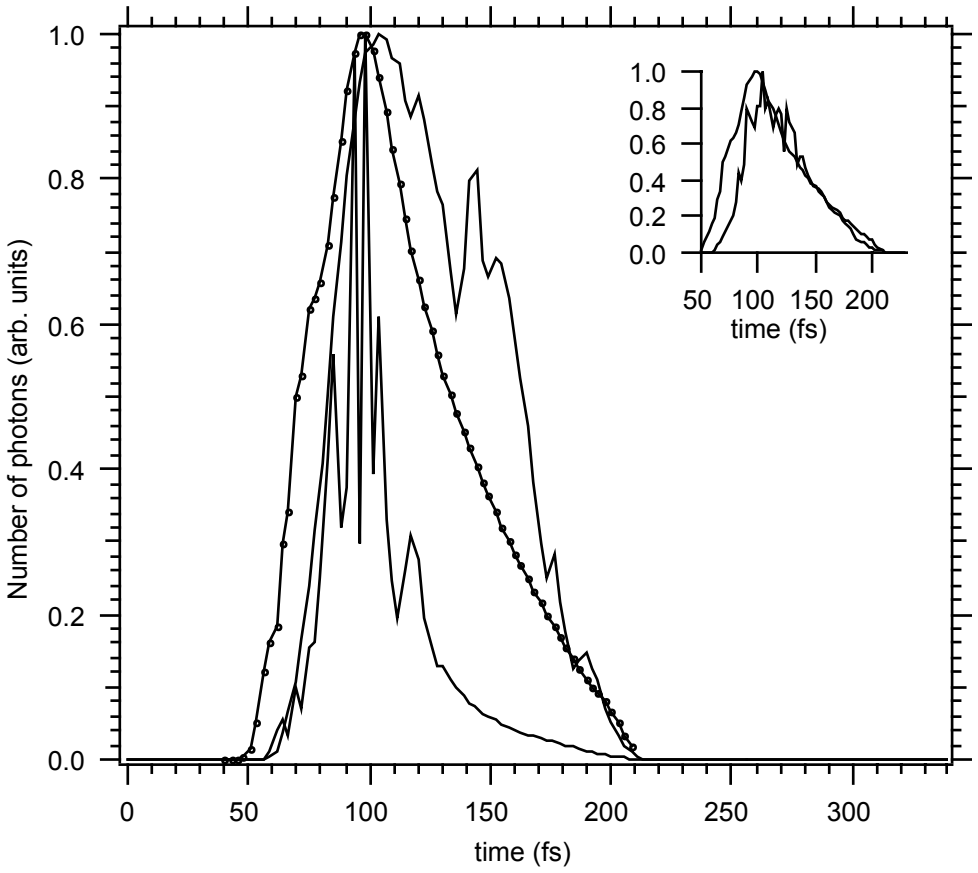
Number of photons (arb. units)
time (fs)
0.0
0.2
0.4
0.6
0.8
1.0
0
50
100
150
200
250
300
50 100 150 200
time (fs)

Figure 5

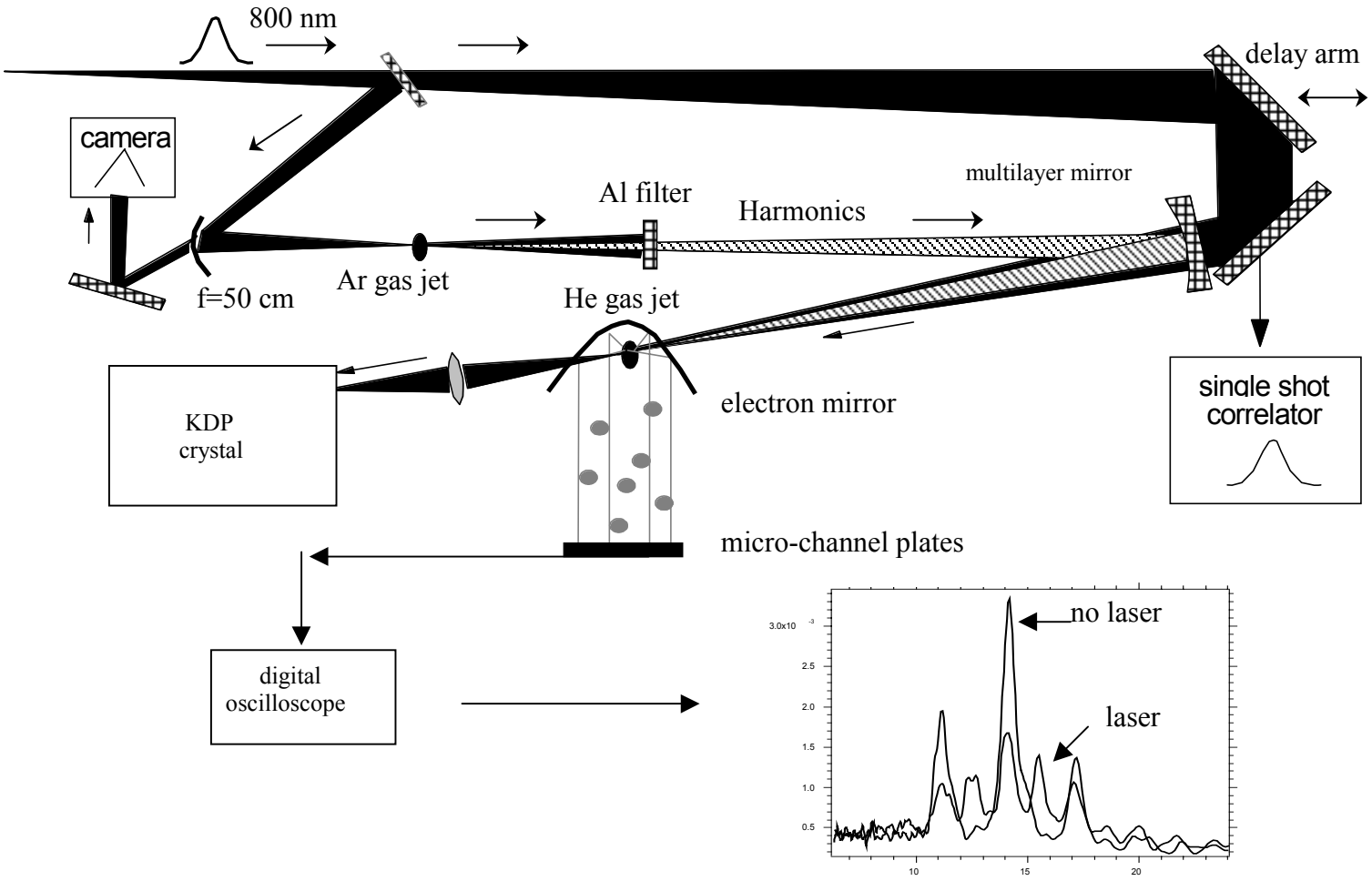
800 nm
delay arm
camera
multilayer mirror
Al filter
Harmonics
Ar gas jet
f=50 cm
He gas jet
KDP
crystal
electron mirror
single shot
correlator
micro-channel plates
digital
oscilloscope
no laser
laser
3.0x10 -3
2.5
2.0
1.5
1.0
0.5
10
15
20

Figure A1

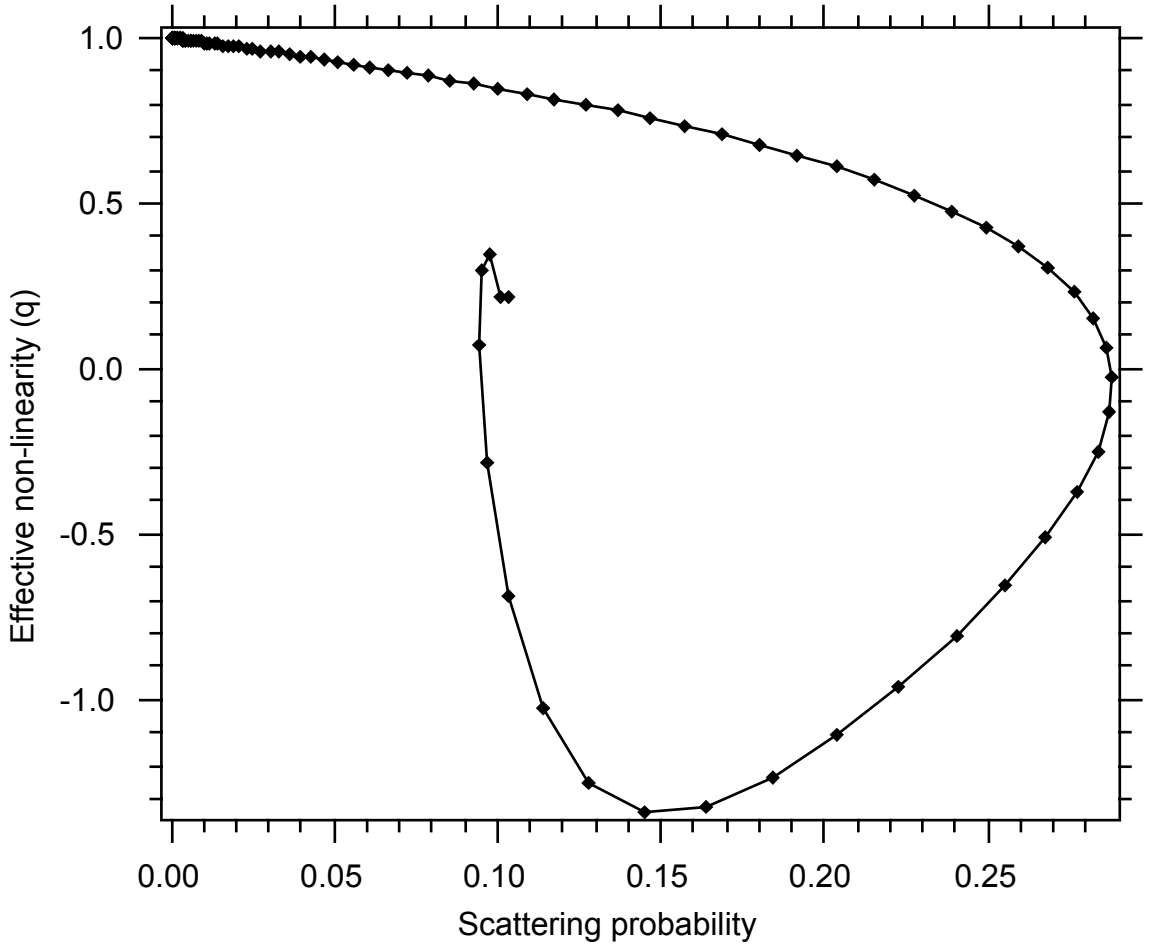
1.0
0.5
0.0
-0.5
-1.0
Effective non-linearity (q)
0.00
0.05
0.10
0.15
0.20
0.25
Scattering probability

Figure A2